Composites Science and Technology 142 (2017) 180–188

Contents lists available at ScienceDirect

Composites Science and Technology

journal homepage: http://www.elsevier.com/locate/compscitech

# Fully degradable PLA-based composite reinforced with 2D-braided Mg wires for orthopedic implants

Xuan Li [a], Chenglin Chu [a, *], Li Zhou [a], Jing Bai [a], Chao Guo [a], Feng Xue [a], Pinghua Lin [a], Paul K. Chu [b]

[a] School of Materials Science and Engineering, Southeast University, Nanjing, 211189, China
[b] Department of Physics and Materials Science, City University of Hong Kong, Tat Chee Avenue, Kowloon, Hong Kong, China

ARTICLE INFO

*Article history:*
Received 20 June 2016
Received in revised form
11 January 2017
Accepted 14 February 2017
Available online 16 February 2017

*Keywords:*
Polymer-matrix composites (PMCs)
Textile composites
Environmental degradation
Finite element analysis (FEA)
Mechanical properties

ABSTRACT

Fully degradable poly-lactic acid (PLA) is reinforced with 2D-braided magnesium alloy wires (Mg wires or MAWs) for bone fixation devices. The relationship between the mechanical/degradation properties of the composite and microstructural features such as braiding angle, volume fraction, and interface properties is investigated. The biaxial mechanical properties of the composite can be tailored by the microstructure. When the braiding angle is 45°, the composite has the highest shear and impact strength and increasing the volume fraction simultaneously improves the tensile, bending, shear, and impact strength. Results obtained by the finite element method show that the screw hole undermines the safety factor of the composite under micro-strain. Acidic degradation of pure PLA can be mitigated by the corporation of MAWs and a degradation model is proposed to predict the mechanical properties of the composite during immersion. Our results reveal a relationship between the bending strength, molecular weight, and immersion time.



## 1. Introduction

Plates and screws as the internal fixation devices play significant roles in restoring and reconstructing the normal activity of fractured bones. Originally, these devices are made of metals such as stainless steels and titanium alloys [1], but metals typically have moduli 5 to 10 times larger than that of cortical bone [2,3] thus producing the well-known stress-shielding effect [4]. Hence, polymer-based composites having low stiffness and high fatigue strength have been proposed as alternatives for internal bone fixation devices [5,6].

With the regards to the revolution of implant materials, two characteristics are desired for the polymer based composite besides compatibility. One is the composite could fully degrade and the strength loss could match the strength increase of the surround tissues during the implantation. Previously, most reported composites are non- [7,8] or partially- [9] degradable. As a result, secondary injure occasionally occurs during the removal of the implants after the bone healing. The other desired characteristic for the composite is that the biaxial mechanical properties could be optimized to bode different bone fixation. For instance, the composite would be anisotropic for weight-bearing bones, while be isotropic for craniofacial and maxillofacial bones. In this respect, textile reinforcement includes two-dimensional (2D) or three-dimensional (3D) fiber reinforcement attracts huge interests, comparing to unidirectional reinforcement. It has been shown that the composites reinforced with textile reinforcements have high impact damage resistance and fracture tolerance under multiple loads and are suitable for bone fixation devices [7,8]. For instance, polyetheretherketone (PEEK) based composites reinforced with braided carbon fibers (CF) have been used as bone plates in femur or tibia fixation [7,8].

Previously, we noticed the feasibility of degradable magnesium alloy wires (MAWs) for the reinforcing of degradable poly-lactic acid (PLA) [10,11]. Then, in this work, 2D-braided MAWs (2D-MAWs) were employed to prepare fully degradable composites. Since the mechanical properties of the composites are related to the structure, it is important to investigate the influence of the various microstructural features. Moreover, micro-strain is necessary for bone growth during healing [12,13], the sensitivity of the braided composite to screw holes under micro-strain is then studied by the finite element method (FEM). Additionally, the degradation

* Corresponding author.
*E-mail address:* clchu@seu.edu.cn (C. Chu).

http://dx.doi.org/10.1016/j.compscitech.2017.02.013
0266-3538/

behavior of the composite is addressed quantitatively and the relationship between the bending strength, PLA molecular weight, and immersion time in simulated body fluids (SBF) is evaluated.

## 2. Materials and methods

### 2.1. Materials preparation

Magnesium alloy wires (MAWs) with a diameter of 0.3 mm (AZ31: 96% Mg, 3% Al and 1% Zn by weight) were used as reinforcements and PLA (PLA: Natureworks LLC) with density of 1.24 g/cm$^3$ was used as the matrix. The fabrication process of the braided composite is illustrated in Fig. 1. The first step involved nailing tacks on a thin polytetrafluoroethylene plate at a distance determined by the unit rhombic cell of the two-dimensional (2D) braided MAWs. The 2D braided MAWs were fabricated manually. The MAWs were braided by a 1/1 interlocking form in which a wire bundle passed over and under a wire yarn at a braiding angle ($\theta$), as shown by the upper right picture in Fig. 1. The interlocking angle between the fill and warp yarn was twice the braiding angle. Thereafter, the PLA/chloroform solution was poured onto the braided MAWs. After evaporating the PLA/chloroform solution, the tacks were plucked and the polytetrafluoroethylene plate was removed to obtain the pre-impregnating braided composite lamina. Afterwards, three pre-impregnating braided composite laminas and four pure-PLA laminas were alternatively stacked and heat-compressed at 165 °C and 2.6 MPa. Braided composites with four different braiding angles 15°, 30°, 45°, 60° and the same volume fraction and those with four different volume fractions of 5%, 7%, 10%, 12% of MAWs but the same braiding angle were prepared. The pure PLA samples were prepared under the same conditions. The specimen dimensions were 120 mm × 12 mm × 2.5 mm.

### 2.2. Mechanical tests

Tensile tests along the longitudinal direction (ASTMD790-2010), three-point bending tests (ASTM D638-03), and shear tests [10] along the transverse section were conducted at room temperature and 5, 2, 5 mm/min cross-head speed, respectively, on the CMT4503 electronic universal testing machine. The Charpy impact test was performed on the unnotched samples along the transverse section on the ZBC impact testing machine.

### 2.3. Micro arc oxidization

Micro-arc oxidization (MAO) is the common method to improve the degradation properties of magnesium alloys. Moreover, it could introduce coarse and porous surface coating on magnesium alloys which may enhance the adhesion between MAWs and PLA. The details of MAO process can be found in the previous paper [14].

### 2.4. Finite element analysis

The isotropic properties and mechanical sensitivity of the composite to holing were assessed by the finite element method (FEM) using the Ansys software. The braiding angle of the composite model in FEM was 45°. The material parameters of PLA and MAWs for FEM can be found in previous paper [10]. The interface between the MAWs and PLA was theoretically treated as complete bonding.

The model and hole parameters are shown in Fig. 2. Two holes were modeled: one breaking the continuity of braided MAWs (denoted as breaking-hole form) and the other not breaking the continuity by adjusting the braiding form (denoted as no-breaking-hole form) as shown in Fig. 2(c) and (d). The corresponding braided

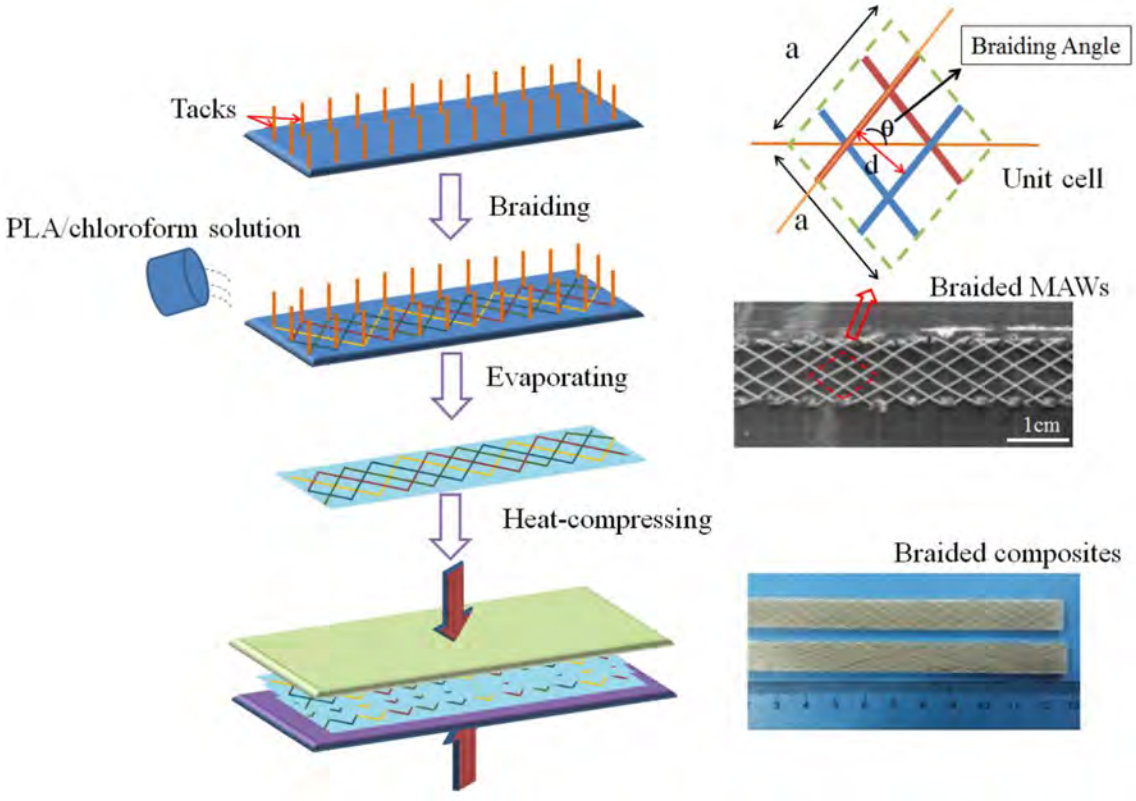


**Fig. 1.** Schematic illustration of the fabrication process and micro-structural features of the braided MAWs/PLA composite.

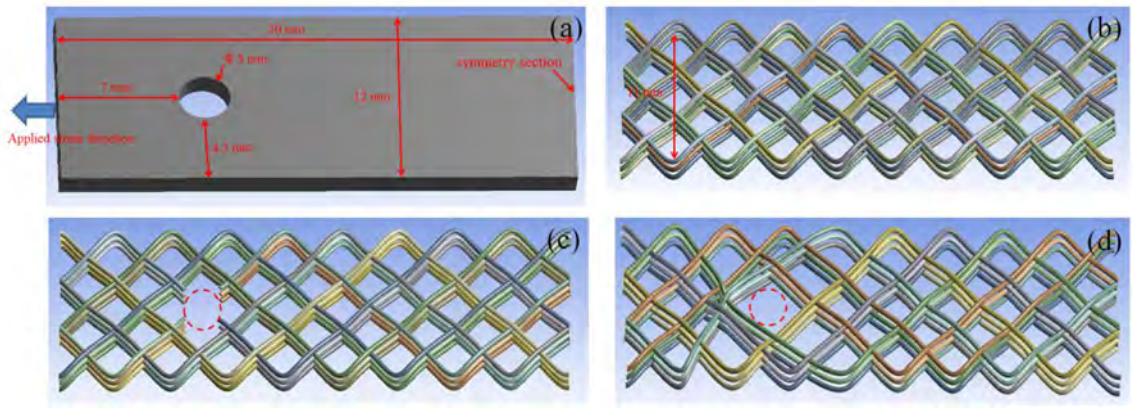


**Fig. 2.** Illustration of the braided composite model in FEM: (a) PLA matrix with a hole; (b) braided MAWs with no hole; (c) breaking-hole form; (d) no-breaking-hole form.

composites were denoted as BC-composite and C-composite. To simplify the calculation, half of the plate (length of plate = 60 mm for bending tests) with a hole was modeled. The thickness and width of the model were 2.5 mm and 12 mm, respectively. In order to provide sufficient protection on the MAWs, the width of PLA matrix (12 mm) was larger than that of braided MAWs (11 mm).

### 2.5. Immersion tests

The composites with dimensions of 60 mm × 12 mm × 2.5 mm used in the immersion tests were reinforced by MAO-treated MAWs (denoted as MAO-composite). The individual samples were placed in 50 ml screw-top plastic bottles and fully immersed in simulated body fluids (SBF) [15] at 37 °C. The solution was changed daily and the bending properties of the wet specimens were determined after immersion for 7, 14, 28, and 56 days. After the bending tests, the samples were dried and the viscosity average molecular weight ($M_v$) of the pure PLA and PLA matrix was calculated by the Mark-Houwink-Sakurada formula [16]. In the pH tests, the pH was recorded periodically during immersion. The experimental data was presented by the average of three measurements for each test.

### 2.6. Microstructural characterization

The fracture morphology was examined by scanning electron microscopy (SEM, Philips XL30 FEG) at an accelerating voltage of 20 kV. Before the investigation, the composite and MAWs were sputter-deposited with a thin gold layers to reduce charging.

## 3. Results

### 3.1. Micro-structural features

The impregnated braided composite lamina is constructed by repetitive unit rhombic cells, as shown in the upper right picture of Fig. 1. The parameters of the cell include the braiding angle ($\theta$), rhombic length ($a$), and distance between MAW yarns ($d$). $d$ and volume fraction ($V_m$) of the MAWs in the unit cell can be calculated as follows:

$$d = a^{*}\sin(180-2\theta)/2 \text{ and} \quad (1)$$

$$V_m = 4^{*}a^{*}\pi^{*}0.15^2/(0.6^{*}a^{*}d) = 4^{*}\pi^{*}0.15^2/(0.6^{*}d). \quad (2)$$

The micro-structural parameters of the unit cell for the braided composites are calculated and presented in Table 1. The biaxial mechanical characteristics of the composite are evaluated by FEM. The braiding angle and theoretical volume fraction of the MAWs in the composite model are 45° and 10 vol%, respectively. It should be mentioned that the real volume fraction of the MAWs in the model is only 6 vol%, because the width and thickness of the composite are larger than the theoretical values based on the unit cell as shown in Fig. 2(b). The Young's modulus along the longitudinal and transverse directions of the braided composites are, respectively, 4.49 GPa and 4.71 GPa and they are 6.46 GPa and 4.23 GPa for the 6 vol% unidirectional composite calculated by the mixture rule [17]. The braided composite at $\theta$ of 45° exhibits the isotropic characteristics (see Table 2).

**Table 1**
Micro-structural parameters of the unit cell of the braided composites.

| Braiding angle (°) | $d$ (mm) | $a$ (mm) | $V_m$ (%) |
|---|---|---|---|
| 15 | 2.35 | 9.4 | 10 |
| 30 | 4.7 | 10.86 | 5 |
| | 3.36 | 7.75 | 7 |
| | 2.35 | 5.43 | 10 |
| | 1.96 | 4.52 | 12 |
| 45 | 2.35 | 4.7 | 10 |
| 60 | 2.35 | 5.43 | 10 |

### 3.2. Micro-structural effects on mechanical properties

#### 3.2.1. Braiding angle effects

The relationship between the mechanical properties and braiding angles for 10 vol% is shown in Fig. 3. The tensile strength ($S_t$) and bending strength ($S_b$) decrease proportionally with $\theta$. According to curve fitting, $S_t$ and $S_b$ of the composite reinforced with the unidirectional MAWs (UD-composite) are approximately 78.7 MPa and 119 MPa, respectively. For a $\theta$ of 60°, $S_t$ and $S_b$ are, respectively, 48.4 MPa and 75.8 MPa and about 61.5% and 63.6% of those of the UD-composite. Furthermore, they are 0.5 and 0.45

**Table 2**
Biaxial Yong's modulus of the braided composite (45°, 10 vol%) derived by FEM and unidirectional composite (6 vol%) by the mixture rule.

| Composite form | Yong's modulus (GPa) | |
|---|---|---|
| | Longitudinal direction | Transverse direction |
| Braided composite | 4.49 | 4.71 |
| Unidirectional composite | 6.46 | 4.23 |

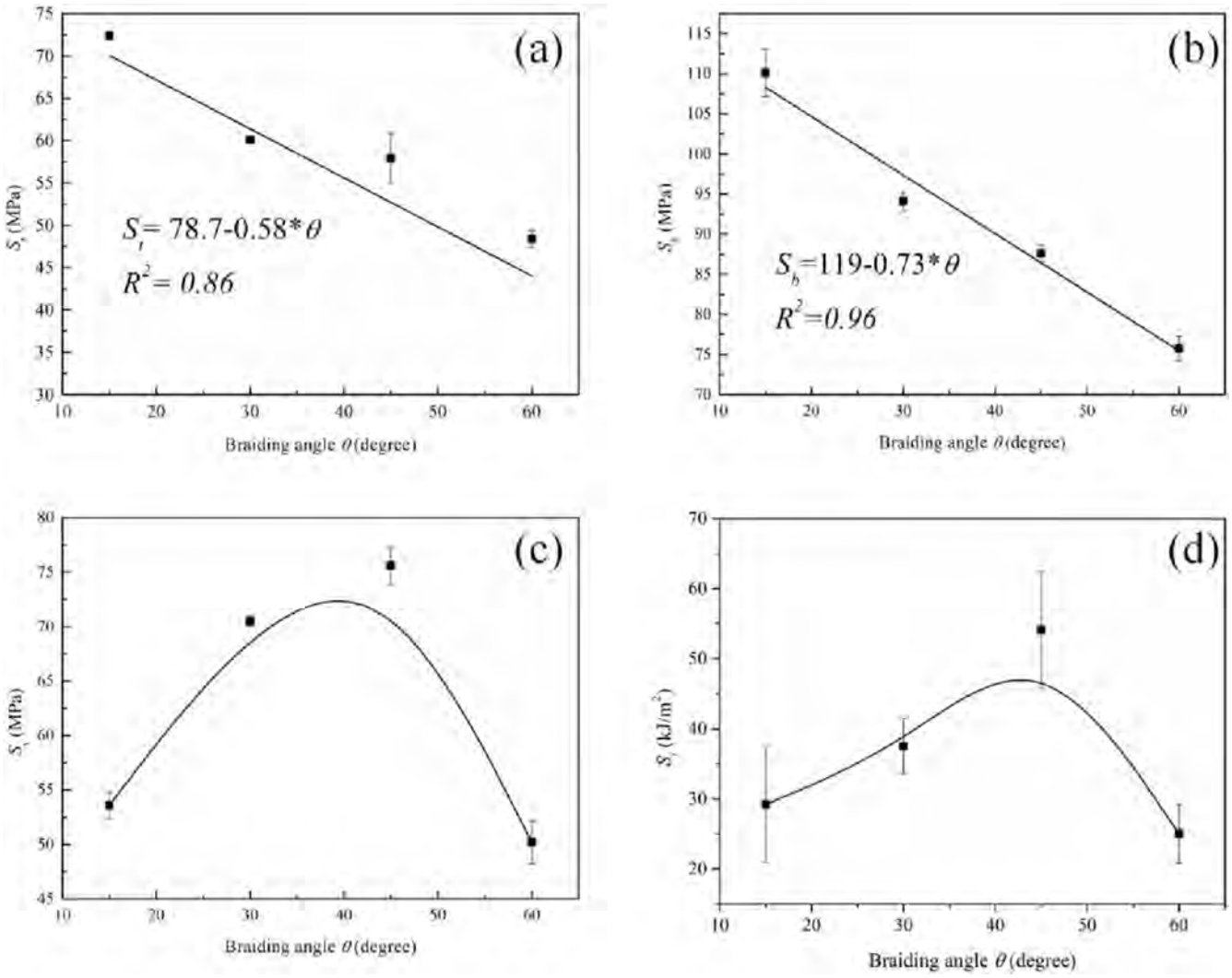


**Fig. 3.** Mechanical properties of the braided composites for different braiding angles at 10 vol%: (a) tensile strength; (b) bending strength; (c) shear strength; (d) impact strength.

times lower than those at 15° and $S_b$ decreases faster than $S_t$ with $\theta$.

The shear strength ($S_s$) and impact strength ($S_i$) increase initially and decrease with $\theta$ being 75.6 MPa and 54.1 kJ/m$^2$, respectively, when $\theta$ is 45°. For comparison, $S_s$ and $S_i$ for $\theta$ of 60° are only 50.2 MPa and 25 kJ/m$^2$ and approximately equal to those for 15°.

### 3.2.2. Volume fraction effects

The mechanical properties of the braided composites for different volume fractions and $\theta$ of 30° are shown in Fig. 4. $S_t$ increases proportionally with $V_m$ and is 68 MPa for 12 vol% but smaller than that for 10 vol% and $\theta$ of 15°, indicating that $S_t$ can be further enhanced by decreasing the braiding angle. The relationship between the measured $S_b$ and $V_m$ is shown in Fig. 4(b). The composite shows a parabolic increase in $S_b$ with $V_m$ and for 12 vol%, $S_b$ is 120 MPa and nearly 1.7 times that of pure-PLA. Similarly, $S_s$ and $S_i$ of the composite increase with $V_m$ from 46 MPa and 17 kJ/m$^2$ for pure-PLA to 80 MPa and 46 kJ/m$^2$ at 12 vol%.

### 3.2.3. Interface effects

The interface influences the mechanical properties of the composite. Here, MAO is performed to modify the MAWs and $S_t$ and $S_s$ of the composite for $\theta$ of 30° after modification are shown in Fig. 5. $S_t$ and $S_s$ increase after MAO and the interface strengthening effect of $S_t$ is more apparent at large $V_m$. For instance, for $V_m$ of 12 vol%, the increase in $S_t$ after MAO is about 20% and about 13% for $V_m$ of 5 vol%. However, with regard to $S_s$, the increase rate is only 3% for $V_m$ of 12 vol% and smaller than that for $V_m$ of 5 vol%. The morphologies at the fractured section of the composite after tensile and shear tests are shown in Fig. 6. The pristine MAW is pulled out from the matrix whereas the MAO-MAW adheres to the matrix after tensile tests as respectively shown in Fig. 6(a) and (b). In the shear test, the PLA matrix near the pristine MAW breaks but the interface between the MAO-MAW and PLA matrix remains integrated after the test as respectively shown in Fig. 6(c) and (d) furnishing experimental verification of interfacial strengthening by MAO.

### 3.2.4. Hole effects under micro-strain

In clinical practice, screw holes are drilled into the composite plates. The holes change the continuity of the reinforcements affecting the properties of the composite. Here, two types of holes are studied including breaking and non-breaking ones. A safety factor (SF), calculated by dividing the real stress with the ultimate tensile strength is adopted to evaluate the mechanical sensitivity of the composite to the hole under a micro-strain of 0.1%.

The results are shown in Fig. 7. The symmetrical section is fixed during the calculation resulting in a small SF of the local PLA matrix.

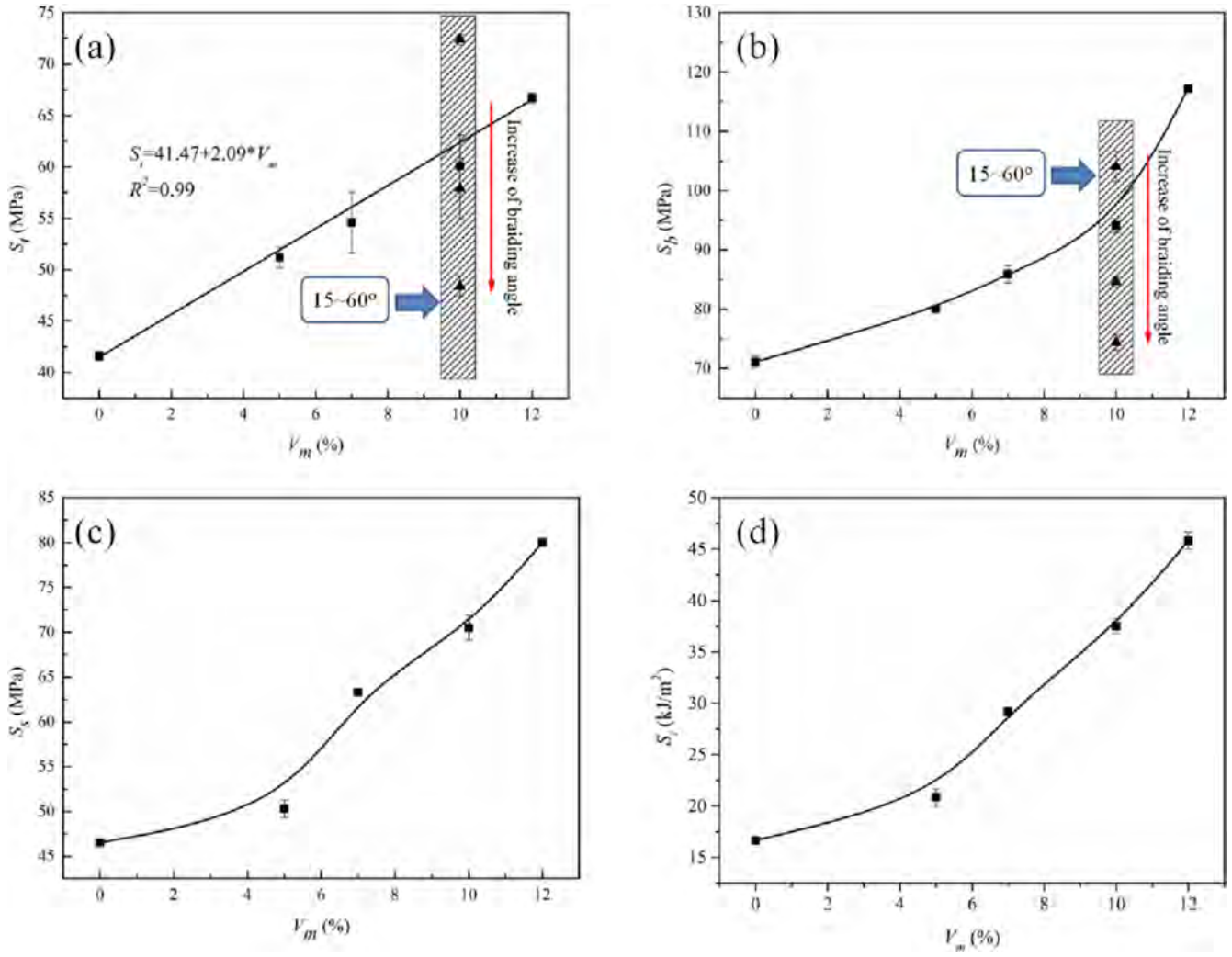


**Fig. 4.** Mechanical properties of the braided composites for different volume fractions and $\theta$ of 30°: (a) tensile strength; (b) bending strength; (c) shear strength; (d) impact strength.

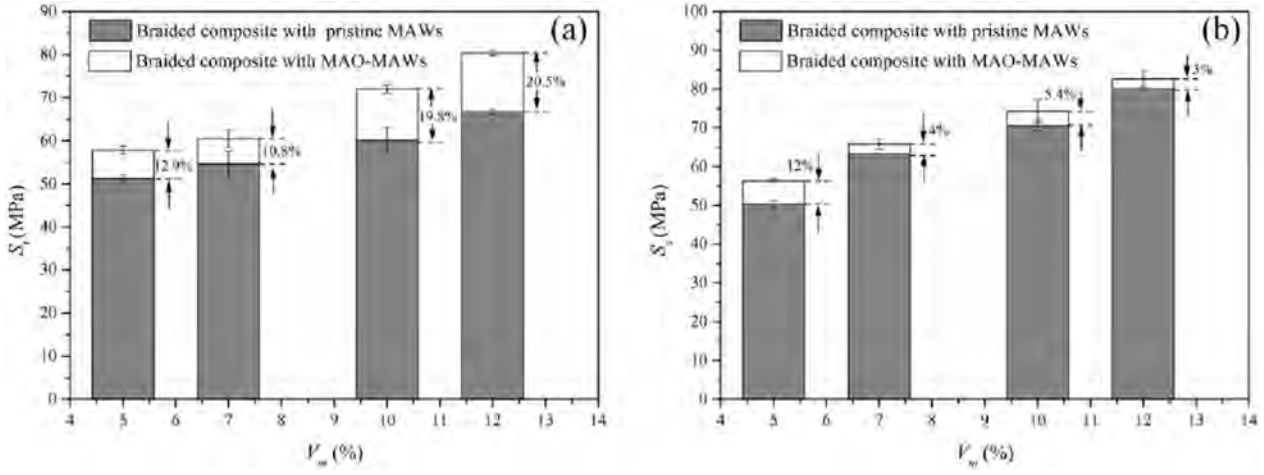


**Fig. 5.** $S_t$ (a) and $S_s$ (b) of the braided composite for $\theta$ of 30° before and after interface modification by MAO.

For pure PLA, the hole decreases the SF of the matrix from 7.8 to about 3.11 indicative of deteriorating safety. With regard to the composite without a hole, SF of the PLA matrix is about 8.78 and larger than 7.8. Meanwhile, the MAWs in the composite have non-uniform SF, and the SF is smaller at the bent locating implying that the stress distributes non-uniformly along the wire and is

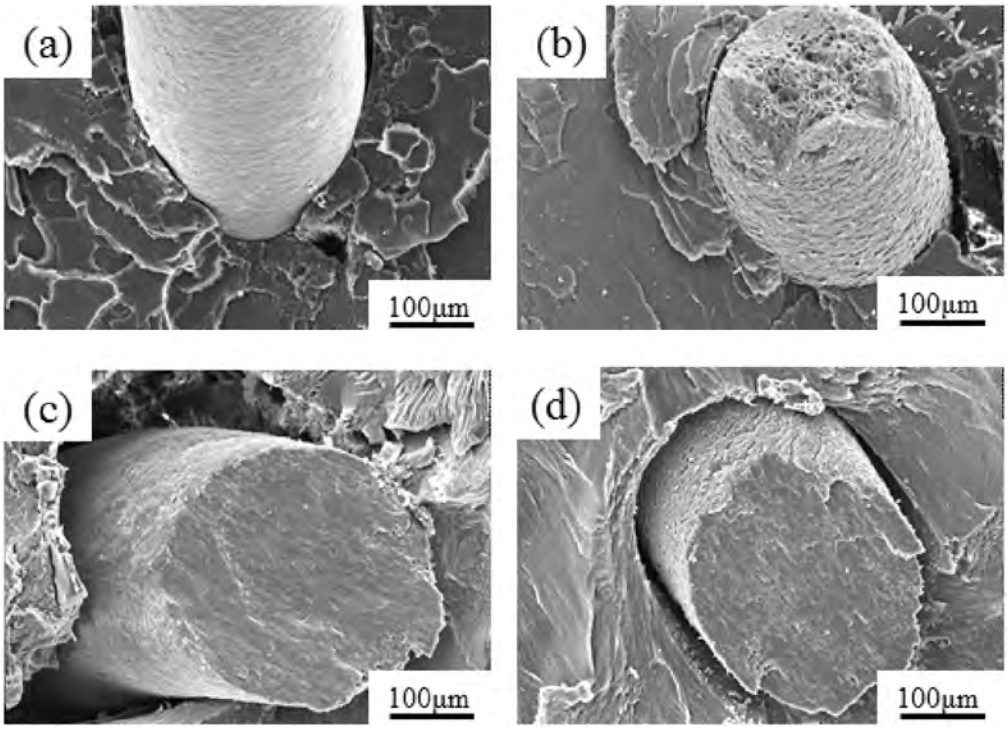


**Fig. 6.** Morphologies of the fractured section of the braided composite after tensile and shear tests: (a) braided composite with pristine MAWs after the tensile test; (b) braided composite with MAO-MAWs after the tensile test; (c) braided composite with pristine MAWs after the shear test; (d) braided composite with MAO-MAWs after the shear test.

concentrated at the bent locations. After the hole is drilled, the SF of the PLA matrix near the hole decreases significantly. The smaller SFs of the matrix near the hole are about 2.83 and 2.78, respectively, for BC-composite and C-composite. The smaller SF of the latter may indicate that the PLA matrix near the hole can sustain a larger load in the case of the non-breaking hole under the same micro-strain. Moreover, in the C-composite, the MAWs around the hole have smaller SF than the other MAWs, indicating worse safety during fixation. The fixed support loads for 0.1% strain of the composite with no hole, BC-composite, are C-composite are respectively 134.74 N, 130.04 N, and 132.24 N.

### 3.3. Degradation of the braided composite

The pH change of the fluid during immersion is displayed in Fig. 8 (a). For pure-PLA, the pH decreases gradually with immersion time denoting acidic degradation. For the braided composites, the pH decreases in the first 3 days and afterwards, it increases slightly and then decreases. For $\theta$ of 30°, the pH of the immersion fluid for 12 vol% is higher than that for 7 vol%. Similarly, for 10 vol%, the pH of the fluid for $\theta$ of 45° is higher than that for $\theta$ of 15°. With regard to the composite at $\theta$ of 30° and 7 vol% [denoted as composite (30°, 7 vol%)], the pH of the fluid is appropriate compared to that for $\theta$ of 15° and 10 vol%.

The $S_b$ changes in the composite (30°, 7 vol%) and pure-PLA are shown in Fig. 8 (b). After immersion for 56 days, $S_b$ is 56 MPa and 56.3% of the initial value. For comparison, $S_b$ of pure-PLA is 31 MPa and about 44% of its initial value. The braided composite has better strength retaining ability. The molecular weight changes of the PLA during immersion are shown in Fig. 8 (c). $M_v$ of pure PLA decreases more quickly than that of the PLA matrix. After immersion for 56 days, $M_v$ of pure PLA is about $3 \times 10^4$ g/mol and that of the composite (30°, 7 vol%) is $4 \times 10^4$ g/mol.

After dissolving PLA matrix by chloroform solution, The surface morphologies changes of MAWs in the composite (30°, 7 vol%)) during immersion are investigated, as shown in Fig. 9. The initial surface of MAO is porous as shown in Fig. 9(a). After 1 week immersion, local pore size increases denoting the degradation of MAO coating, as shown in Fig. 9 (b). As the immersion proceeded, the porous characteristics disappeared and the coarse surface exposed, suggesting the breakage and fully degradation of MAO coating as shown in Fig. 9(c), (d) and (e).

## 4. Discussion

### 4.1. Mechanical characteristics

Plates and screws are widely used in bone fixation surgery. In order to overcome the “stress-shielding effects”, composite-based plates have been investigated as possible replacements for metallic plates but most of these efforts have focused on unidirectionally (UD) laminates and discontinuous short fibers as the reinforcements. Our previously reported UD fiber composite [10] offers high strength and stiffness along the fiber direction, but suffers from low strength in the direction perpendicular to the fibers, while composites with discontinuous short fibers have low strength. Therefore, compared to these materials, the composite investigated here would represent balanced mechanical properties along the transverse and longitudinal direction. Although the studied composite has lower strength than that with carbon fibers [9] due to the small $V_m$ in the reinforcements and low $M_v$ in the matrix, the fully degradable characteristic of the composite bodes well for craniofacial and maxillofacial bones whose tensile and bending strengths are low and about 70 MPa [18] and 120 MPa [19], respectively. Moreover, as shown by our results, the mechanical properties can be tailored by the braiding angle, volume fraction, and interface modification.

In practice, screw holes are produced in the plates and they

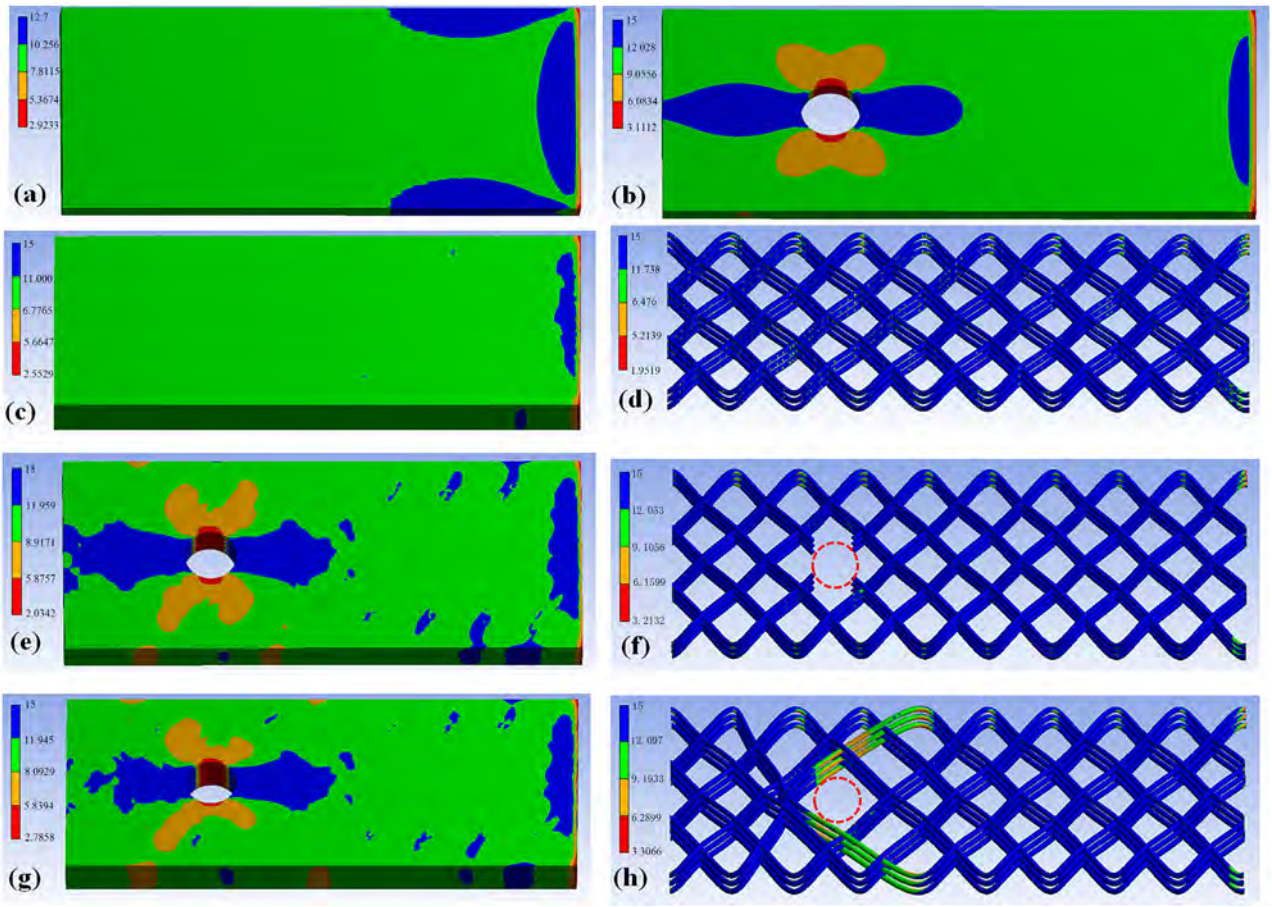


**Fig. 7.** Safety factor of pure PLA and braided composites under a micro-stain of 0.1%: (a) pure-PLA without a hole; (b) pure-PLA with a hole; (c) PLA matrix in the braided composite without a hole; (d) MAWs in the braided composite without a hole; (e) PLA matrix in the BC-composite; (f) MAWs in the BC-composite; (g) PLA matrix in the C-composite; (h) MAWs in the C-composite.

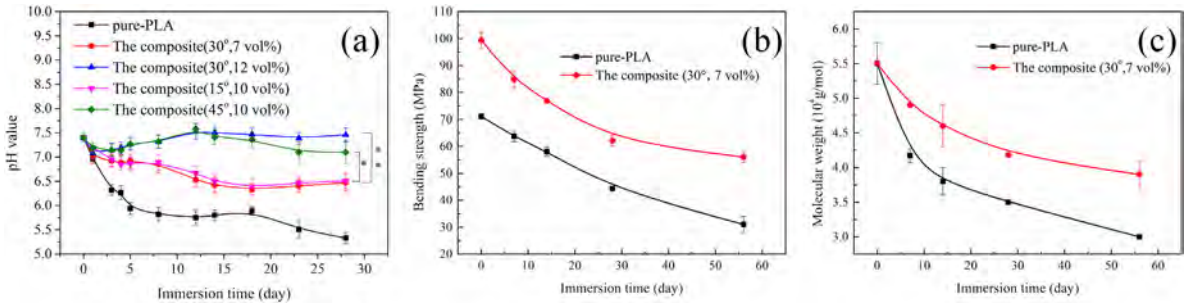


**Fig. 8.** Degradation behaviors evolution of pure PLA and the braided composite during immersion: (a) pH changes in the fluid; (b) $S_b$ changes; (c) $M_v$ changes.

normally adversely affect the mechanical properties of the composite. In order to reduce the influence, the reinforcements are commonly braided bypassing the hole to retain the fiber continuity [7]. This type of non-breaking holes enhances the safety compared to the breaking ones under the same load. However, when a constant strain is applied, the non-breaking reduces the safety factor of the reinforcement. This effect should be considered in the design of the materials and fixation devices.

### 4.2. Degradation kinetics

It is well known that degradation of PLA would release acidic products and decrease the pH, which may induce the inflammation. In this work, degradation of MAWs releases alkaline products to counteract the pH decrease forming a compensating relationship between the PLA and MAW. The process also depends on the braiding angle and volume fraction. During braiding, the MAWs and coating experience large plastic deformation at the bent locations, which may possibly lead to the partial breakage of the coating. This breakage would be more apparent while increasing the strain and immersion time [20]. Hence, the solution has a larger pH for the composite with a larger braiding angle for the same volume fraction after immersion for 28 days.

Moreover, MAWs fillers reduce the decrease of $M_v$ of the PLA matrix and $S_b$ of the composite. An approximately linear relationship between the reciprocal of the polymer molecular weight and

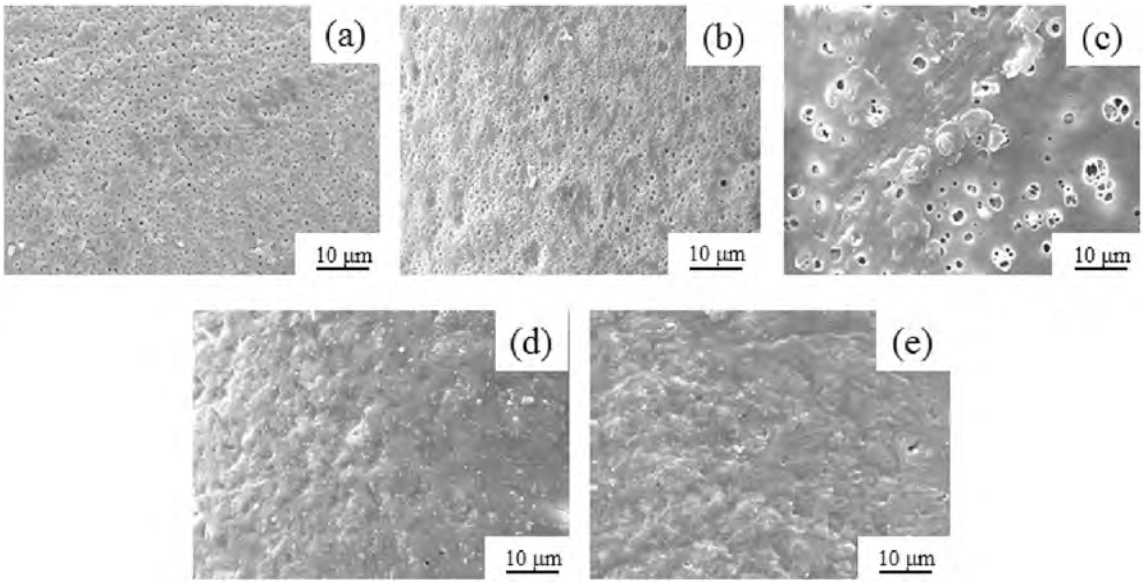


**Fig. 9.** Surface morphology changes of MAWs in the composite (30°, 7 vol%) versus immersion time: (a) initial; (b) 1 week; (c) 2 weeks; (d) 4 weeks; (e) 8 weeks.

degradation time is observed from the pure-PLA and composite (30°, 7 vol%) and the trend is consistent with the hydrolytic degradation theory of PLA [21], as shown in Fig. 10(a). The decrease in $M_v$ can be evaluated as follows:

$$\ln M_v = A - kt, \tag{3}$$

where $A$ is a constant value and $k$ is the hydrolysis rate. Curve fitting yields $A$ and $k$ of 10.77 and 0.0091, respectively, for pure-PLA and 10.85 and 0.0056 for the PLA matrix in the composite. The hydrolysis rate constant $k$ of pure PLA is 0.63 times larger than that of PLA in the composite, suggesting that pure PLA degrades faster than the PLA matrix in the composite.

During the implantation, the composite is expected to have suitable mechanical properties with the tissues and so it is significant to know $S_b$ of the composite for a given immersion time or given $M_v$. A relationship between the fracture strength $\sigma$ and number average molecular weight $M_n$ of a polymer has been proposed as follows [22]:

$$\sigma = \sigma_\infty - B/M_n, \tag{4}$$

where $\sigma_\infty$ is the fracture strength for a finite molecular weight and $B$ is a constant value. In our study, we notice $S_b$ of pure PLA and the composite also exhibits a linear relationship with $1/M_v$ as shown in Fig. 10(b) as follows:

$$\text{Pure-PLA: } S_b = 125.28 - 2.74 \times 10^6/M_v, \tag{5}$$

$$\text{Composite (30°, 7 vol%): } S_b = 206.77 - 5.96 \times 10^6/M_v. \tag{6}$$

Dividing Eq. (4) by Eqs. (5) and (6), respectively, produces the relationship of $S_b$ with time as follows:

$$\text{Pure-PLA: } S_b = 125.28 - 2.74 \times 10^6 \times \exp(0.0091 \times t - 10.77), \tag{7}$$

$$\text{Composite (30°, 7 vol%): } S_b = 206.77 - 5.96 \times 10^6 \times \exp(0.0056 \times t - 10.85). \tag{8}$$

Fig. 10(c) shows the simulated curves based on Eqs. (7) and (8) in the predetermined immersion period as well as the experimental results. The simulated results agree well with the experimental ones, suggesting that the degradation model for bending strength is valid.

### 4.3. Feedback to the braided composite

In this work, the main objective is to introduce a fully degradable composite to different bone fixation devices and formulate a

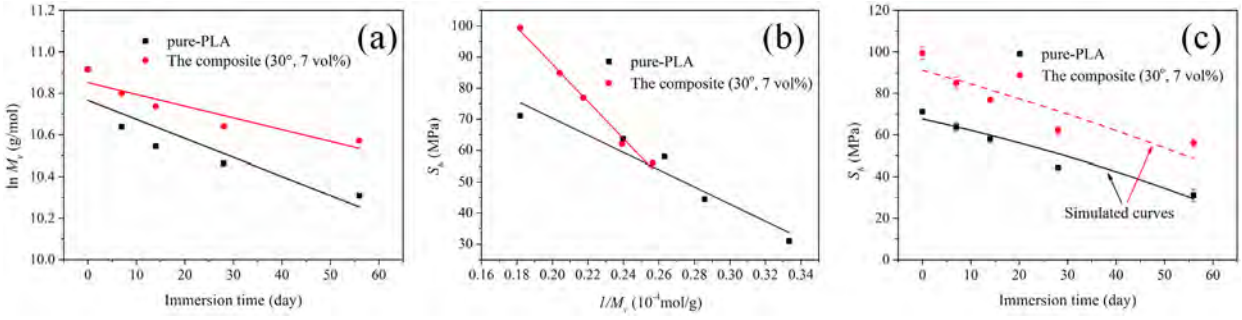


**Fig. 10.** Degradation properties of pure PLA and the braided composite during immersion: (a) ln $M_v$ versus immersion time; (b) $S_b$ versus $1/M_v$; (c) simulated curves of $S_b$ of pure PLA and the braided composite (30°, 7 vol%) versus immersion time.

quantitative model to predict the mechanical properties of the composite during immersion. According to the results, the mechanical properties could be significantly improved by increasing $V_m$. Thus, a high $V_m$ is needed for high strength. However, owing to the relatively large diameter of the MAWs (0.3 mm compared to about 7 μm of a carbon fiber), a higher $V_m$ may suggest a thicker plate. Therefore, more efforts need to be devoted to the preparation of smaller diameter MAWs. Moreover, biaxial mechanical properties of the composite could be minutely tailored by the braiding angle to meet the different requirements on biaxial mechanical properties and $\theta$ of 45° is preferred for high shear or impact resistance. Additionally, the mechanical properties of PLA depend on the molecular weight. In this work, they are smaller than those in clinical use, suggesting that the properties and strength retention ability can be further improved by using PLA with a larger molecular weight.

It should be mentioned that the proposed model on $S_b$ is not applicable to immersion for a very long time because as immersion proceeds, the degradation kinetic of PLA may deviate from the first-order kinetics [23]. Nevertheless, this equation is useful to quantitative analysis of the micromechanical environment between the implants and fractured bones during healing, as the first-order reaction is valid for a long time (about 250 days in phosphate buffered saline (PBS) at 37 °C [24] and longer than the normal healing time of about 3 months).

## 5. Conclusion

Fully degradable PLA-based composites reinforced with 2D-braided magnesium alloy wires are produced for orthopedic bio-applications. The biaxial mechanical properties of the composite can be tailored by the braiding angle, volume fraction, and interface modification. Holes drilled into the devices decrease the safety factor of the composite and *in vitro* tests reveal the compensatory relationship between PLA and MAWs pertaining to the degradation behavior of the composite. A degradation model is proposed to predict the bending strength of the composite with immersion time and reveals a well-defined relationship between the bending strength, molecular weight, and immersion time.

## Acknowledgements

This work was jointly supported by the National Natural Science Foundation of China (Grant No. 31570961), State Key Program of National Natural Science Foundation of China (Grant No. 51631003), National Key Research and Development Program of China (Grant No. 2016YFC1102402), Scientific Research Foundation of Graduate School of Southeast University (YBJJ1525), Jiangsu key laboratory for advanced metallic materials (BM2007204), and Hong Kong Research Grants Council (RGC) General Research Funds (GRF) No. CityU 11301215.

## References

[1] Y.F. Zheng, X.N. Gu, F. Witte, Biodegradable metals, Mater. Sci. Eng. R. 77 (2014) 1–34.
[2] Y. Chen, Z. Xu, C. Smith, J. Sankar, Recent advances on the development of magnesium alloys for biodegradable implants, Acta Biomater. 10 (2014) 4561–4573.
[3] K.J.L. Burg, S. Porter, J.F. Kellam, Biomaterial developments for bone tissue engineering, Biomaterials 21 (2000) 2347–2359.
[4] D.R. Sumner, J.O. Galante, Determinants of stress shielding: design versus materials versus interface, Clin. Orthop. Relat. Res. 274 (1992) 202–212.
[5] T. Kasuga, Y. Ota, M. Nogami, Y. Abe, Preparation and mechanical properties of polylactic acid composites containing hydroxyapatite fibers, Biomaterials 22 (2000) 19–23.
[6] H. Mehboob, S.-H. Chang, Evaluation of healing performance of biodegradable composite bone plates for a simulated fractured tibia model by finite element analysis, Compos Struct. 111 (2014) 193–204.
[7] K. Fujihara, Z.-M. Huang, S. Ramakrishna, K. Satknanantham, H. Hamada, Performance study of braided carbon/PEEK composite compression bone plates, Biomaterials 24 (2003) 2661–2667.
[8] K. Fujihara, E. Yoshida, A. Nakai, S. Ramakrishna, H. Hamada, Influence of micro-structures on bending properties of braided laminated composites, Compos. Sci. Technol. 67 (2007) 2191–2198.
[9] Y.Z. Wan, Y.L. Wang, Z.R. Wang, F.G. Zhou, J.Y. Xin, C3D/PLA composite—a promising material for osteosynthesis devices, J. Mater Sci. Lett. 19 (2000) 1207–1210.
[10] X. Li, C.L. Chu, L. Liu, X.K. Liu, J. Bai, C. Guo, et al., Biodegradable poly-lactic acid based-composite reinforced unidirectionally with high-strength magnesium alloy wires, Biomaterials 49 (2015) 135–144.
[11] X. Li, C. Guo, X. Liu, L. Liu, J. Bai, F. Xue, et al., Impact behaviors of poly-lactic acid based biocomposite reinforced with unidirectional high-strength magnesium alloy wires, Prog. Nat. Sci. Mater. 24 (2014) 472–478.
[12] J. Kenwright, T. Gardner, Mechanical influences on tibial fracture healing, Clin. Orthop. Relat. Res. 355 (1998). S179–S90.
[13] S.M. Perren, Evolution of the internal fixation of long bone fractures, J. Bone Jt. Surg. Br. 84 (2002) 1093–1110.
[14] C.L. Chu, X. Han, J. Bai, F. Xue, P.K. Chu, Surface modification of biomedical magnesium alloy wires by micro-arc oxidation, T Nonferr. Metal. Soc. 24 (2014) 1058–1064.
[15] T. Kokubo, H. Takadama, How useful is SBF in predicting in vivo bone bioactivity? Biomaterials 27 (2006) 2907–2915.
[16] A. Schindler, D. Harper, Polylactide. II. Viscosity–molecular weight relationships and unperturbed chain dimensions, J. Polym. Sci. Pol. Chem. 17 (1979) 2593–2599.
[17] R.M. Jones, Mechanics of Composite Materials, CRC press, Boca Raton, 1998.
[18] J.H. McElhaney, J.L. Fogle, J.W. Melvin, R.R. Haynes, V.L. Roberts, N.M. Alem, Mechanical properties of cranial bone, J. Biomech. 3 (1970) 495–511.
[19] J.A. Motherway, P. Verschueren, G. Van der Perre, J. Vander Sloten, M.D. Gilchrist, The mechanical properties of cranial bone: the effect of loading rate and cranial sampling position, J. Biomech. 42 (2009) 2129–2135.
[20] R. Vayeda, J. Wang, Adhesion of coatings to sheet metal under plastic deformation, Int. J. Adhes. Adhes. 27 (6) (2007) 480–492.
[21] S. Song, A.M. Waas, K.W. Shahwan, X. Xiao, O. Faruque, Braided textile composites under compressive loads: modeling the response, strength and degradation, Compos. Sci. Technol. 67 (2007) 3059–3070.
[22] I.M. Ward, J. Sweeney, Mechanical Properties of Solid Polymers, John Wiley & Sons, New York, 2012.
[23] V. Piemonte, F. Gironi, Kinetics of hydrolytic degradation of PLA, J. Polym. Environ. 21 (2013) 313–318.
[24] Schley J. Lyu, B. Loy, D. Lind, C. Hobot, R. Sparer, et al., Kinetics and time–temperature equivalence of polymer degradation, Biomacromolecules 8 (2007) 2301–2310.